J Solid State Electrochem (1998) 2: 181–190

ORIGINAL PAPER

Matthew Denesuk · Donald R. Uhlmann

Phenomenological analysis of the optoelectrochemical behavior of electrochromic intercalation devices

Received: 17 April 1997 / Accepted: 2 September 1997

Abstract A set of phenomenological analysis tools have been developed for the characterization of the optoelectrochemical behavior of electrochromic intercalation devices. Both step current and step potential excitations are considered. Great simplification is afforded by working with the passed charge as the primary independent variable; consideration is also given, however, to the transmission or built-in device potential as independent variables. It is shown that quasi-static intercalation efficiency curves, generated from step current measurements, can elucidate the intercalation site-energy distribution; these curves are also compared to dynamic intercalation efficiency curves obtained from step potential measurements. Quasi-static and dynamic optical efficiencies are also considered and compared. The scaling properties of some of the phenomenological parameters may be used to generate master curves which unify sets of data obtained under a variety of conditions (applied voltages, imposed currents, film thicknesses, etc.). Quantitative predictions can be made of device behavior under conditions not probed experimentally.

Key words Electrochromism · Intercalation · Device · Phenomenological analysis

List of symbols

A_λ, T_λ, R_λ:	absorbance, transmittance, and reflectance, respectively, at wavelength, λ
j, j_0:	time-dependent current, constant current, respectively
J, J_0:	charge-dependent current, current at $\Delta Q = 0$, respectively
L:	film thickness
ΔQ, ΔQ_f, ΔQ_{max}:	instantaneous change in passed charge, final passed charge, maximum attainable passed charge, respectively
R, R_0, ΔR:	intrinsic device resistance, initial device resistance, and added series resistance, respectively
V_a, V_0, V_{bi}:	applied, initial, and built-in potentials, respectively
x, Δx:	fractional intercalation level, change in the fractional intercalation level, respectively
η, η_0:	driving potential and initial driving potential, respectively
ξ_λ, $\hat{\xi}_\lambda$:	optical efficiency and dynamic optical efficiency, respectively, at wavelength, λ
ζ_λ, $\hat{\zeta}_\lambda$:	intercalation efficiency and dynamic intercalation efficiency, respectively, at wavelength, λ

M. Denesuk (✉) · D.R. Uhlmann
Arizona Materials Laboratories,
Department of Materials Science and Engineering,
University of Arizona, Tucson, AZ 85712, USA
Tel.: +1-520-322-2963; Fax: +1-520-322-2993
e-mail: mdenesuk@u.arizona.edu

Introduction

The object of the present paper is to present a set of phenomenological analysis tools and demonstrate their application to characterization of the behavior of electrochromic (EC) intercalation devices. The use of specific models is avoided as much as possible. This type of analysis can be very useful: based upon the behavior of the device under one set of conditions, behavior under another set of conditions can often be predicted with impressive accuracy. In addition, the results of phenomenological analysis provide important directions for the development of specific mechanistic models.

A large number of electrochromic intercalation materials and device configurations have been investigated, and a variety of specific models have been variously proposed; a useful review of these is provided in two recent texts [1, 2]. Because no comprehensive physical

picture or model of device behavior has emerged, there is great value in a comprehensive system of phenomenological analysis tools. The present paper presents a set of such tools and demonstrates their application to some representative sets of data. Details of the experiments from which the representative data are taken are given in [3–6]. Where appropriate, such details (intercalation host thickness, electrolyte concentration, reference electrode, imposed current, applied potential, etc.) are given in the figure captions.

Basic physical picture

Although the present analysis is substantially independent of specific physical models, it is helpful to proceed with a general physical picture of the device being analyzed. Such a device is typically of the form:

e^--conductor/intercalation host/ion conductor/intercalation reservoir/e^--conductor

where the *ion conductor/intercalation reservoir* pair often take the form of a single material structure. Application of a potential, V_a, between the two e^--conductors results in transport of the intercalate species from either the reservoir to the host or vice versa. For an electrochromic device, this transport results in a change in the optical properties of at least one of the components of the device. The transport continues until either the device is open-circuited or until a built-in potential, V_{bi}, sufficient to counteract V_a is generated by the components between the e^--conductors. This picture may be represented schematically as Fig. 1.

Closing the circuit (imposing V_a) induces intercalate transport between the reservoir and the host. As the host fills with intercalate, its optical properties change and V_{bi} increases. Transport continues until either the circuit is opened or until $V_{bi} \approx V_a$; $V_a - V_{bi}$ $(\equiv \eta)$ may be seen as a driving force for the intercalation process. When the host empties (as by application of a reverse voltage), V_{bi} decreases and the optical properties change (in a sense opposite to that which takes place as the host fills).

The experiment

In a typical experiment, a particular form of V_a is imposed, and the time evolution of selected device properties is measured as the device relaxes to a new state. A variety of forms for V_a are used; the most common are step potential (chronoamperometry), triangle wave (cyclic voltammetry), and step current (chronopotentiometry). In the latter, a feedback loop within the supply modifies V_a in whatever manner is necessary to maintain a constant electrical current.

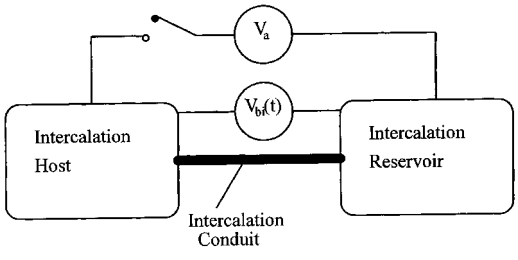

Fig. 1 Schematic phenomenological model of intercalation system

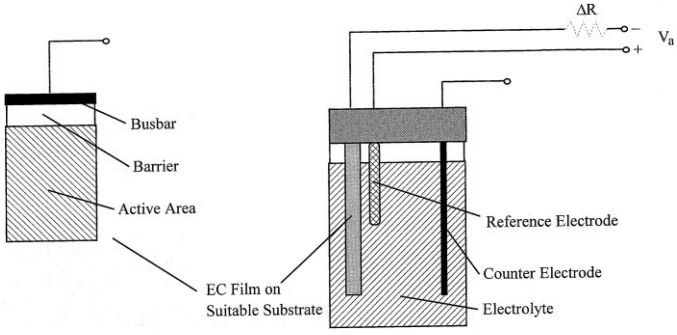

Fig. 2 Schematic representation of the EC device used to obtain the data which are used in the present paper

Presently, we consider step current and step potential excitations. For the step current measurement, the current density through the device is raised (essentially instantaneously) from $j = 0$ to a constant value, $j = j_0$, and the time-dependent potential, $V_a(t)$, necessary to maintain that current is measured along with the optical transmission, $T(t)$. $V_a(t)$ is measured relative to a reference electrode in the ion conductor. Detailed analysis of this kind of experiment, along with extensive data for H-intercalation, is given in [3, 4]. For the step potential measurement, the potential is changed (also essentially instantaneously and relative to a reference electrode in the ion conductor) from its initial value, V_0, to a new value, V_a, and the time-dependent current, $j(t)$, and the optical transmission, $T(t)$, are measured. A reference electrode is used in these measurements so that processes involving the reservoir do not complicate the analysis, and so that results may directly be compared among different investigators.

A schematic representation of the device used to generate the data which is used in the present paper is given in Fig. 2. Both aqueous (for H-intercalation) and non-aqueous (for Li-intercalation) electrolytes were used. The active area of the film, determined by an attached barrier, was typically $\sim 2.5 \times 3.5$ cm^2. When a series resistor, ΔR, is used, it is inserted in series with the potential, V_a, thereby reducing the actual potential between the EC film and the reference electrode. Some details of the experiments are given in the appropriate figure captions, and a full description is presented elsewhere [3–6].

The device behavior may be affected by a number of variables. Those discussed in the present work are: (a) applied potential, V_a; (b) imposed current density, j_0; (c) film thickness, L; (d) series resistor, ΔR (in series with the EC device); and (e) insertion species, M (presently H or Li).

The analysis

Analysis of step current experiments

Total passed charge, ΔQ

For a constant current density, j_0, the total charge passed, ΔQ, is given by:

$$\Delta Q = j_0 \cdot t \tag{1}$$

If leakage, side currents, and/or fluxes contribute only negligibly to j_0, ΔQ should be proportional to the change

in the intercalation level of the host. In the present discussion, if this restriction is fulfilled, the current is said to be *pure*. In addition, if j_0 is sufficiently small relative to the rate of intercalate redistribution within the host, ΔQ should determine the instantaneous change in state of the electrode; if this restriction is fulfilled, the behavior is said to be *quasi-static*. It is often useful to consider device properties as functions of ΔQ.

The intercalation *level* is represented by the *ratio* of the number of filled intercalation sites to the total number of intercalation sites and is often designated in the literature as x. For a pure current, we may represent the change in intercalation level, Δx, as:

$$\Delta x \approx \frac{\Delta Q}{\Delta Q_{\max}} \tag{2}$$

where $\Delta Q_{\max}$ is the maximum *attainable* passed charge (not the maximum attained). Although an estimate of $\Delta Q_{\max}$ is not readily obtainable without using a specific model, its scaling properties are expected to be relatively straightforward.

Δx may be taken as the actual intercalation level, x, only if the change is large relative to the initial level ($\Delta x \gg x_o$). The experimental conditions can often be controlled to ensure that this condition is at least roughly satisfied.

Transmission, T

Electrochromic intercalation devices are of interest primarily because of the changes which can be made, reversibly and controllably, in their optical properties. In a typical experiment, the transmission, T, and/or the reflectance, R, are measured at a particular wavelength, λ, or over some range of wavelengths. In dynamic studies, the transmission at a single wavelength, T_λ, is by far the most commonly measured property. A typical T_λ (ΔQ) plot, obtained for several j_0-values, is shown in Fig. 3 (see [3, 6]). The fact that the curves coincide quite closely while the current is varied by nearly a factor of 4 indicates that kinetic factors are not important over this range of conditions.

Optical efficiency, ξ_λ. The average optical efficiency (often called the coloration efficiency [1]) is defined as the ratio of the change in optical density to the amount of charge passed to bring about that change, and represents the average slope of the log $T_\lambda - \Delta Q$ plot. If log T_λ is linear in ΔQ, the optical efficiency is constant, and the ratio calculation is clearly meaningful. It is more common, however, that log $T_\lambda - \Delta Q$ is nonlinear (as in Fig. 3), and the average optical efficiency varies continually with intercalation. In such cases, it is useful to define the optical efficiency, ξ_λ[cm^2/C], as

$$\xi_\lambda = \left| \frac{\partial \log T_\lambda}{\partial \Delta Q} \right| \tag{3}$$

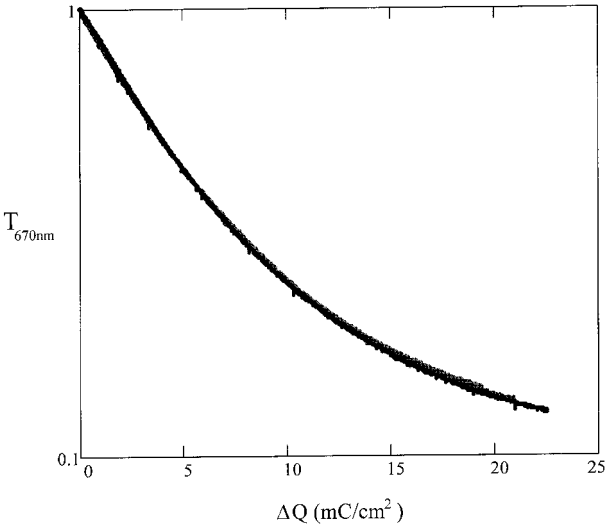

Fig. 3 The $\log_{10}$-scaled transmission, T_λ, as a function of the passed charge, ΔQ, for three values of the imposed current, j_0 (j_0 = 11, 5.7, 2.9 μA/cm^2). The device is based on a 1950 Å WO_3 film with an Li-electrolyte (0.01 M $LiClO_4$ in dry propylene carbonate). See [3, 6]

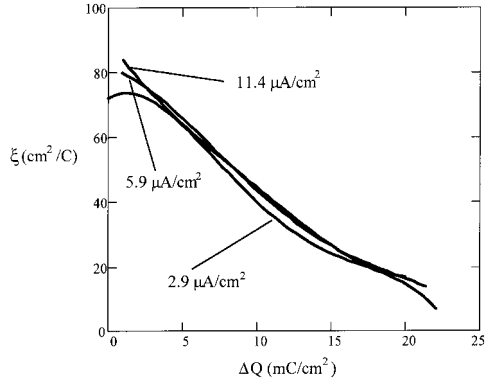

Fig. 4 The optical efficiency, ξ_λ, as a function of passed charge, ΔQ, based on the data shown in Fig. 3

Quasi-static $\xi_\lambda(\Delta Q)$ curves, calculated from the log $T_\lambda - \Delta Q$ curves in Fig. 3, are shown in Fig. 4. It is notable that the optical efficiency continually decreases with increasing intercalation.

Analysis of optical data. Extraction of relevant parameters from $T_\lambda(\Delta Q)$ is complicated primarily by four factors: (1) thin film interference effects, (2) lack of knowledge of the reflectance behavior, $R_\lambda(\Delta Q)$, (3) impure currents, and (4) non-quasi-static conditions. Factors (3) and (4) are more likely to be important at higher currents, such as those often occurring under typical constant voltage conditions.

For typical film thicknesses and scales of homogeneity, thin film interference effects may be significant and variable at visible wavelengths. For sufficiently broadband optical measurements, these effects may "average out." Under monochromatic conditions, however, the measured $T_\lambda(\Delta Q)$ may be specific to the precise film

thicknesses and wavelength used; to extract parameters of general utility, therefore, it is necessary to consider directly the effects of thin film interference.

Methods for calculating the optical properties of thin-film stacks with known thicknesses, L_i and complex indices, $\tilde{n}_i$ ($\equiv n_i + ik_i$), are widely known [7, 8], but the inverse problem is not readily solvable in a unique way. It is therefore useful to use a model for $\tilde{n}_i$ representing the active layers; the parameters may be varied iteratively to approximate the measured data. The resulting modelled $\tilde{n}_i$ may then be used (tentatively) to predict T and R for other device configurations.

The second issue [lack of knowledge of $R_\lambda(\Delta Q)$] can be addressed by measuring the reflectance during the experiment, but this is not commonly done (primarily because of the additional experimental requirements). If one performs the modelling mentioned above with regard to thin film interference effects, $R_\lambda(\Delta Q)$ may be estimated. It should be noted, however, that in the optical range, the reflectance is typically expected to vary not nearly as much as the absorbance. Generally, therefore, variations in T_λ will be due primarily to changes in the absorbance, A_λ, and not in R_λ. It should also be noted that, for many applications, one may want a phenomenological parameter which lumps together the reflection and absorption effects.

Applied potential, V_a

Before proceeding with methods of electrical potential analysis, it is important to identify the physical significance of the measured potential, V_a, which is the voltage necessary to maintain a fixed current, j_0. In the general case, it may be said that the current is an increasing, homogeneous function of the difference between the applied and some built-in device potential, $V_a - V_{bi}$. It therefore follows that V_a approximates to V_{bi} as the magnitude of the current approaches zero. In practice, we may make stronger statements. It seems quite likely that, at very small values, the current is roughly a linear function of $V_a - V_{bi}$ (which corresponds to an ohmic process with proportionality constant, $1/R$, where R is a device resistance). We therefore have

$$V_a = V_{bi} + jR \tag{4}$$

i.e., V_a is equal to V_{bi} plus a (small) ohmic drop (and the latter varies linearly with the imposed current). If R is independent of the intercalation level, V_{bi} is readily obtained; if R varies, one can attempt to describe it explicitly or one can choose j sufficiently small that jR is negligible.

The built-in potential, $V_{bi}(\Delta Q)$. From the above section, it is seen that, under appropriate conditions, one may estimate the time dependence of V_{bi} from a basic step current measurement. It is often useful to plot the estimated V_{bi} as a function of ΔQ. For a given film, one generally expects V_{bi} to be a master function of ΔQ;

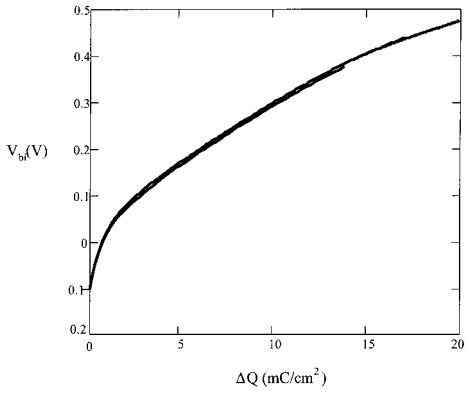

Fig. 5 The estimated built-in device potential, V_{bi}, as a function of the passed charge, ΔQ for three values of the imposed current, j_0 (j_0 = 0.11, 0.22, 0.44 mA/cm^2). The device is based on a 2250 Å WO_3 film in an aqueous electrolyte (0.01 N H_2SO_4); the potentials are vs an Ag/AgCl reference electrode. See [3, 5]

thus, *as long as the current is small enough in magnitude, V_{bi} should not depend upon j_0* (quasi-static conditions). An example, for several different j_0 values, is shown in Fig. 5 (see [3, 5]). It is seen that the three curves are effectively indistinguishable, indicating that, for this range of j_0, the device is ohmic, and polarization and/or intercalate redistribution processes are not important (or even noticeable). The device appears to be in the quasi-static limit under the conditions indicated.

It is important to note that for a given form of site energy distribution, V_{bi} is expected to be a unique function of the intercalation level, x (phenomenologically represented as $\Delta Q/\Delta Q_{max}$). Thus, if one changes only the *number* of sites (by changing the host thickness, for example), the curve should be proportionally scaled. In the case of variations in thickness, if $\Delta Q_{max} \propto L$ (i.e, the general character of the intercalation sites does not change with the film thickness), a plot of V_{bi} vs $\Delta Q/L$ should generate a master curve.

It is also possible that, for a given film, cycling affects the number of available sites. If this is the case, and if the energy distribution of intercalation sites remains relatively unchanged, a set of V_{bi} curves should be scaleable to a master curve (V_{bi} vs $\Delta Q/\Delta Q_{max}$) with a reasonable variation of ΔQ_{max}.

It is important to note the distinction between the number of sites and the form of the distribution. A given film can contain several different types of sites, and the measured distribution will be a composite of these. Changes to the system may affect differently the different components represented in the distribution, and simple scaling behavior may not be observed; in such a case it is necessary to scale appropriately the affected component(s) of the distribution. It should also be noted that processes not directly contributing to intercalation (polarization charging, leakage, for example) can contribute to the measured distribution. The form of the energy distribution can be investigated by considering the intercalation efficiency (below).

Intercalation efficiency, ζ. Adopting an approach similar that used for obtaining the dynamic optical efficiency from the variation of transmission with intercalation, we can obtain an *intercalation efficiency*, ζ, from the variation of ΔQ with V_{bi}:

$$\zeta \equiv \left| \frac{\partial \Delta Q}{\partial V_{bi}} \right| \tag{5}$$

In a literal sense, ζ represents the amount of charge which is passed for a given change in the built-in device potential (and is therefore effectively a differential capacitance). Under quasi-static conditions, however, the passed charge should be directly proportional to the intercalation level, x, of the electrode, and $\zeta/\Delta Q_{max}$ gives directly the change in x for a given potential variation, $\partial x/\partial V_{bi}$. Given the elusiveness of ΔQ_{max}, however, and in keeping with the phenomenological spirit of the present analysis, we shall use ζ alone as a measure of the intercalation efficiency.

If one plots ζ against V_{bi}, a measure of the distribution of available site energies is obtained. If the curve is relatively featureless, there is likely a continuous distribution of site energies; if there is a fine structure (peaks, kinks, humps, etc.), then there are likely discrete types of sites separated significantly in energy. Figure 6 shows a typical $\zeta(V_{bi})$ plot that displays a fine structure.

The hump (centered around 0.2 V) and the peak (centered around 0.45 V) likely indicate the centers of two different site distributions, possibly present in two different phases (TEM micrographs of this tungsten oxide film indicate at least three distinct phases [9]). It appears that a third distribution may be probed at higher potentials. If one is willing to make assumptions regarding the form of the site distributions, decomposition into constituent distributions may be attempted.

Regarding the spacing and scale of the distributions, it should be noted that the V_{bi} axis may also be seen as an energy axis, where the voltage values are numerically the same as the relative energy values in units of eV.

The presence of a *distribution* of site energies imposes another constraint on the definition of quasi-static conditions. The filling of sites of different energies may occur with different characteristic time constants. At sufficiently high intercalation rates, therefore, the evolution of the distribution may vary with the rate, and quasi-static conditions may not prevail.

Transmission-potential plots. It may also be useful to investigate the behavior of T_λ (or $\log T_\lambda$) vs the estimated V_{bi}. This circumvents many of the problems associated with estimating the intercalation level from the passed charge; under quasi-static conditions, T_λ and V_{bi} should be functions only of the intercalation level of the host (non-intercalation fluxes should have little effect on them). Additionally, the problem of the offset (replacing x with Δx) is no longer present.

Because the filling of different types of sites may impact the optical properties differently, however, it may in some cases not be possible to avoid consideration of individual components of the distribution. A typical plot for several j_0 values is given in Fig. 7. It is seen that the three curves are virtually indistinguishable, indicating that, for currents in this range, there is a unique correspondence between built-in potential and transmission.

It may also be useful to investigate the behavior in T_λ-V_{bi} space over full intercalation-deintercalation cycles (allow $j_0 < 0$) to see if any hysteresis is present. Hysteresis in such a plot likely indicates that there is another contribution to V_{bi}.

Analysis of step potential experiments

Step potential analysis is generally more involved than step current analysis, primarily because a wide range of

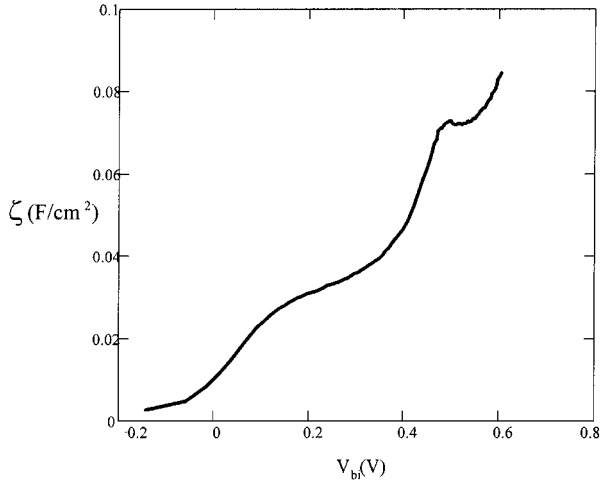

Fig. 6 The intercalation efficiency, ζ, as a function of the built-in potential, V_{bi}. The device is based on a 2250 Å WO_3 film in an aqueous electrolyte (0.01 N H_2SO_4); the potential is vs an Ag/AgCl reference electrode; $j_0 = 0.11$ mA/cm^2

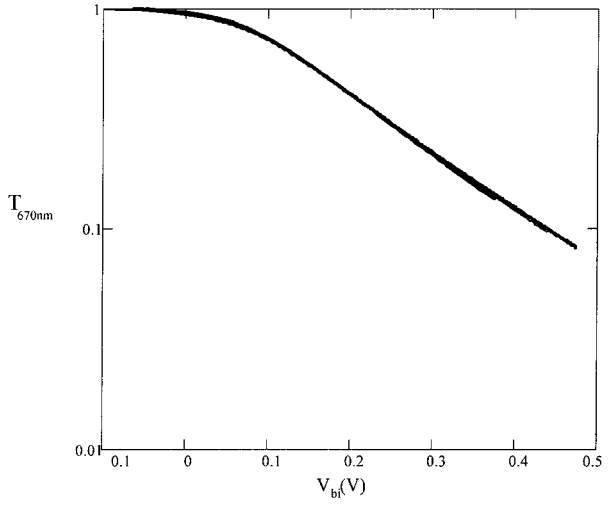

Fig. 7 Log_{10}-scaled transmission, T_λ, as a function of the built-in potential, V_{bi}, based on the data shown in Fig. 5

rates (indicated by the instantaneous current) are probed in a single experiment. Typically, the rate is greatest at the beginning of the experiment and decreases monotonically with time.

As with step current experiments, it is often useful to analyze the measured parameters as functions of the passed charge, ΔQ; one thus obtains $J(\Delta Q)$ and $T_\lambda(\Delta Q)$ plots. The latter are analyzed in essentially the same manner as for the step current measurements; in this case, however, the rate (which corresponds to j_0 in a step current measurement) is initially very large and decreases continually during the experiment. If quasi-static conditions prevail over the entire range of rates, the results should be quite similar to those obtained in slow step current measurements. If this is not the case, the results need to be interpreted in a dynamic context.

Generally, the efficacy of analysis with ΔQ taken as the independent variable lies in the assumption that the processes of interest are state processes, and that they are therefore capable of being parameterized independently of time. Diffusion, for example, is not such a process, and demonstration of ΔQ as a state variable, therefore, would suggest that diffusion is not a limiting mechanism.

Total passed charge, ΔQ

In a step potential measurement, the current is a function of time. Calculation of ΔQ therefore involves an integration:

$$\Delta Q = \int_0^t j(t')\,\mathrm{d}t' \tag{6}$$

An advantage of this type of measurement is that leakage currents may be more easily subtracted from the data. The form of the leakage may be quite complicated, but, as a first approximation, one can assume it is constant and equal to the steady-state current. This current can be subtracted from the measured current, resulting in better estimates of the intercalation current. If the steady state is never reached, one can estimate the corresponding leakage current level via extrapolation.

If J contains other "impurities" (significant non-intercalation contributions such as polarization or complicated leakage, for example), it may be necessary to make further corrections; if conditions are strongly non-quasi-static, it may be necessary to involve time-dependent considerations.

It should be noted that constant-voltage experiments often sample a significantly different range of intercalation level than do constant-current experiments, and this may be a source of discrepancy between the two regarding device properties measured as a function of ΔQ; if ΔQ_0 differs significantly from zero, ΔQ is only a relative measure of intercalation level. To compare properties, the measured curves may need to be shifted in ΔQ such that they begin in initially comparable states. This may be done with the assumption that, for a given type of system, devices are in comparable states when their potentials or transmissions are comparable.

Analysis in $J(\Delta Q)$ space

The capabilities of direct analysis of $j(t)$ curves for intercalation electrodes are generally quite limited. This is because the state of the electrode (indicated by the intercalation level) is changing with time, and the *manner* in which this occurs changes with essentially every controlling variable that may be varied. It is meaningful to investigate comparatively the effect of a controlling variable on the current only if one is comparing currents corresponding to similar electrode states; otherwise there is always an unknown variable present. It is therefore of great benefit to obtain a plot of the current as a function of a variable which indicates the state of the electrode. If the intercalation process is occurring quasi-statically, one can use the transmission, T_λ, or the passed charge, ΔQ. The latter has the advantage that it is expected to correspond more simply to an intercalation level and that its scaling behavior is more straightforward and universal (it is not yet clear how T_λ may scale with L, for example). The former has the advantage that it is measured directly and that it should be independent of leakage, polarization, etc. Both have been used as static indicators of equivalent electrode states (see, for example, [10, 11]). In the present discussion, ΔQ will be used predominantly as the variable indicating the state of the intercalation electrode. It should be noted, however, that comparisons between $J(\Delta Q)$ and $J(T_\lambda)$ plots may help elucidate the influence of factors that affect ΔQ but not T_λ (polarization and leakage currents, for example). It should also be noted that the presence of quasi-static behavior generally implies the absence of diffusion as a limitation.

One can obtain a parametric $J(\Delta Q)$ plot from the elimination of t from $\Delta Q(t)$ and $j(t)$. If two devices begin with comparable initial conditions, it is expected that they are in the same state if they have the same value of $\Delta Q/\Delta Q_{\max}$. This allows one to investigate straightforwardly the effects of various controlling variables (V_a, L, ΔR, M, etc.) on the current. If the initial conditions differ, suitable shifting and/or scaling may be performed before comparison. Although $\Delta Q_{\max}$ is not generally known, its scaling properties are often straightforward; an accurate indicator of the electrode state may therefore be obtained.

A typical transformation from $j(t)$ to $J(\Delta Q)$ space is shown in Fig. 8. Much information may be gleaned from a $J(\Delta Q)$ plot. The y intercept [which is the same as that in $j(t)$ space] gives the initial current, J_0, from which an initial ohmic resistance, R_0, may be calculated:

$$R_0 = \frac{\eta_0}{J_0} \tag{7}$$

where $\eta_0 = V_a - V_0$. If the current is controlled by a constant resistance (as is often believed to be the case

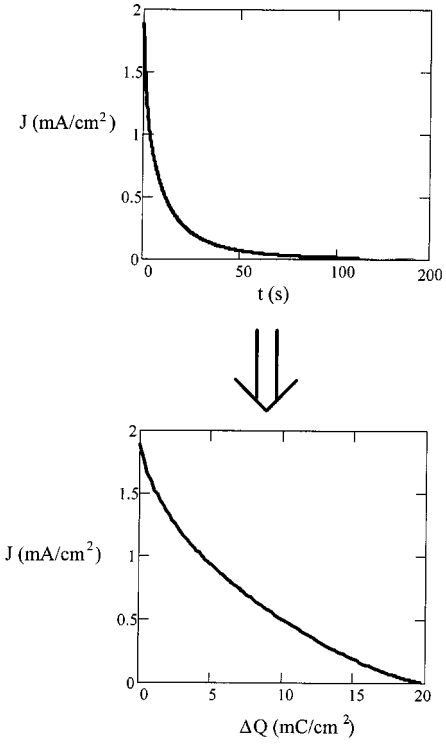

Fig. 8 $j(t) \Rightarrow J(\Delta Q)$ transformation of the intercalation current for a WO_3-based device [1900Å WO_3 film, $V_a = -0.6$ V vs Ag/AgCl ($V_0 \approx 0.0$ V), aqueous electrolyte (0.01 N H_2SO_4)]

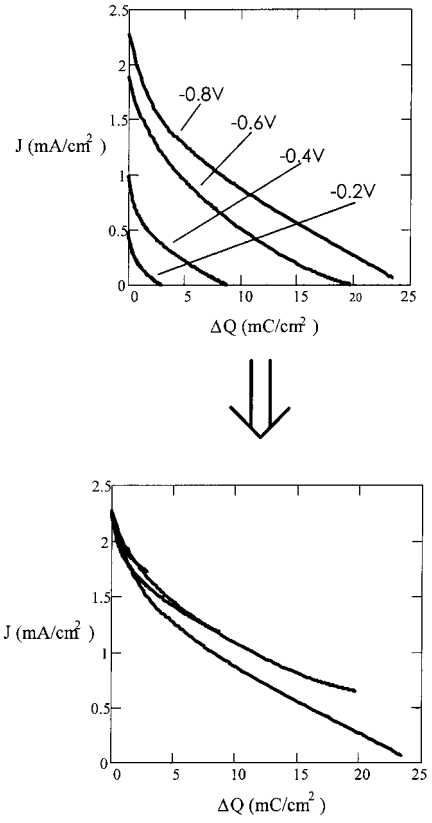

Fig. 9 Collapse of $J(\Delta Q)$ curves obtained from intercalation experiments performed on a WO_3-based device with applied voltages of −0.8 V, −0.6 V, −0.4 V, and −0.2 V vs Ag/AgCl in aqueous electrolyte (0.01 N H_2SO_4); $V_0 \approx 0.0$ V. The WO_3 film is 1900 Å, and the resistances are obtained from the initial currents of each experiment

[10, 11]), then R_0 is the device resistance. Less restrictively, R_0 may be seen as a general kinetic parameter characterizing the dynamic electrical response of the device.

The x intercept gives the *total passed charge*, ΔQ_f. If ΔQ_f is normalized by an appropriate driving parameter (applied voltage, for example), it represents an *intercalation capacity* (which is akin to an average intercalation efficiency, $\bar{\zeta}$). For the data shown in Fig. 8, $R_0 \approx 300\ \Omega\text{cm}^2$ and $\Delta Q_f \approx 19.7\ \text{mC/cm}^2$. Taking η_0, as the driving parameter, the intercalation capacity is $\sim 32.8\ \text{mC V}^{-1}\ \text{cm}^{-2}$.

Master curves. Another advantage of the $J(\Delta Q)$ representation is the facility with which master curves may be generated. Scaling/shifting with system parameters is usually relatively straightforward:

1. Potential scaling: Collapsing of $J(\Delta Q)$ curves corresponding to different applied potentials will depend upon the nature of the controlling process. To effect the collapse empirically, one must ensure that the curves begin with the devices in comparable initial states. For intercalation of a given species, this is most easily accomplished by beginning the experiments at comparable initial potentials; for de-intercalation, this often is not possible, and one must shift the data.

In executing such collapses, it is useful to define a "standard state," i.e., the curve to which the others are to be collapsed. It is often convenient to choose one of the obtained $J(\Delta Q)$ curves as the standard, thereby defining the conditions under which it was obtained as the standard state. Standard state parameters will be indicated with a superscripted "nought": J^0, η_a^0, R^0, etc.

If the current density is controlled by a constant resistance (ohmic process), the potential drop differs from that of the standard state by the difference in initial applied overvoltage: $R^0 J^0 = RJ + \Delta\eta_0$, where $\Delta\eta_0 = \eta_0^0 - \eta_0$. A current, J, may thus be collapsed to the standard state by the operation

$$J^0 = J\frac{R}{R^0} + \frac{\Delta\eta_0}{R^0} \tag{8}$$

If the resistances are the same, the currents are shifted simply by an amount equal to the current corresponding to the difference in initial applied overvoltages. Figure 9 presents an example of a moderately successful collapse brought about by application of Eq. 8.

As another example, if the controlling process is exponential in potential, $J = a\exp(b\eta)$, and if b is independent of potential, the logarithm of the currents obtained at the two different applied overvoltages should be shifted by a linear function of the difference in the applied overvoltages:

$$\ln(J^0) = \ln(J) + \ln\left(\frac{a^0}{a}\right) + b\Delta\eta_0 \tag{9}$$

Exponential scaling does not bring about a reasonable collapse of the curves in Fig. 9.

Insofar as quasi-static and pure conditions are maintained, dynamic $T_\lambda(\Delta Q)$ plots should need no potential scaling/shifting; the curves should simply proceed further at higher potentials. This appears generally to be observed (see the Section "Dynamic optical efficiency, $\hat{\xi}_\lambda$", below). It should be noted, however, that de-intercalation curves must often be shifted to make the initial states comparable.

2. Series resistor scaling: If one adds an external resistance, ΔR, in series with the device, the scaling of the data depends, again, upon the limiting process. Performing a series of experiments with resistors of different value in series with a particular device can therefore be used to elucidate the nature of the limiting processes. The effect of the series resistor is to lessen the average potential dropped across the device without changing the final device potential. Series resistor collapsing may therefore be treated in a manner similar to applied potential collapsing. Taking the current obtained with no series resistor, J_R, as defining the standard state $\left(J_R \rightarrow J^0\right)$, and assuming a resistance-controlled process, one has $R^0 J^0 = \left(R^0 + \Delta R\right)J$. A current, J, may thus be collapsed to the standard state by the operation

$$J^0 = \frac{R^0 + \Delta R}{R^0} J \tag{10}$$

where R^0 is the intrinsic ohmic device resistance (obtained from the standard-state curve). If control by a constant resistance prevails, one may take measurements with several different series resistors to determine R^0. An example of moderately successful ohmic scaling is shown in Fig. 10.

If the controlling process is exponential, one must explicitly subtract the ohmic drop from the overvoltage; a straightforward analysis gives:

$$\ln\left(\frac{J^0}{J}\right) = \ln\left(\frac{a^0}{a}\right) + b\left(\Delta R J - R^0\left[J^0 - J\right]\right) \tag{11}$$

and plotting $\ln\left(\frac{J^0}{J}\right)$ vs $\Delta R J - R^0\left[J^0 - J\right]$ should render a straight line with slope b and intercept $\ln\left(\frac{a^0}{a}\right)$.

As with potential scaling, so long as quasi-static and pure conditions are maintained, the dynamic $T_\lambda(\Delta Q)$ curve should not vary with the addition of series resistors. The nature (or absence) of a variation with ΔR may be used to probe a slow coloration reaction, such as that which has been observed in tungsten oxide films by some workers [10, 11].

3. Thickness scaling: If intercalation occurs equally through the thickness, L, of a given film, and if the intrinsic device resistance is independent of the film thickness, then $J(\Delta Q)$ curves corresponding to films of different thicknesses should collapse to a single curve when plotted as a function of the passed charge *volume density*, $\Delta Q/L$. If the device resistance varies with L, the variations may be treated as additional series resistors and accounted for as described above. Figure 11 displays an example of thickness scaling.

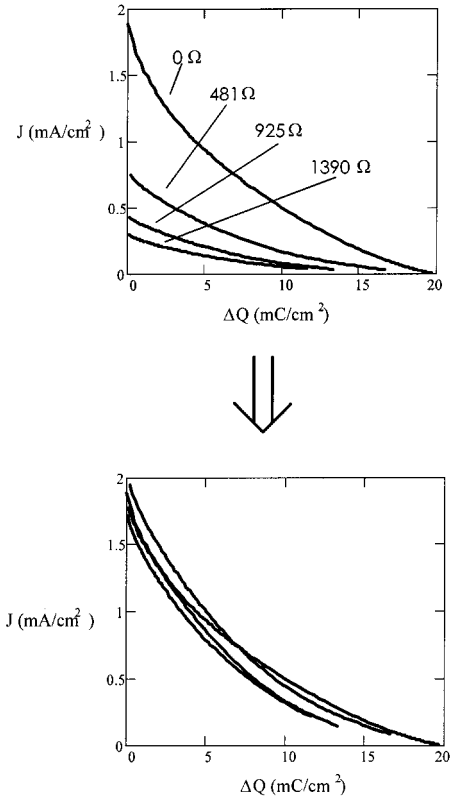

Fig. 10 Ohmic scaling collapse of $J(\Delta Q)$ curves obtained from intercalation experiments performed on a WO_3-based device with series resistors of value 0 Ω, 481 Ω, 925 Ω, and 1390 Ω in aqueous electrolyte (0.01 N H_2SO_4); $V_a = -0.6$ V vs Ag/AgCl, $V_0 \approx 0.0$ V. The WO_3 film thickness is 1900 Å

It is seen that the thickness scaling, with thickness varied by nearly an order of magnitude, brings about a sharp collapse. This indicates that, in a macroscopic sense, intercalation occurs uniformly throughout the WO_3 film and that quasi-static conditions are maintained.

If the actual collapse is dubious, L may be treated as an empirical parameter and varied to bring about the "best collapse"; L then indicates an *effective film thickness* or an *intercalatable film thickness*.

The scaling of dynamic $T_\lambda(\Delta Q)$ plots with thickness should depend upon the optical modulation mechanism(s) and upon the influence of thin-film interference effects.

4. Grand master curves: Using the methods described above, it may often be possible to construct a master curve upon which data obtained under a broad range of experimental conditions collapse. From the parameterization of this curve and a knowledge of the scaling/shifting laws, one then has a broadly applicable, simple mathematical expression which describes the system

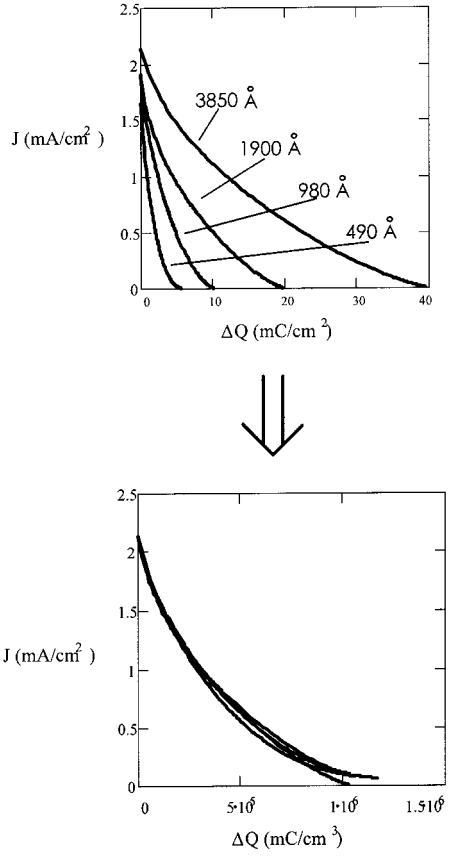

Fig. 11 Collapse of $J(\Delta Q)$ curves obtained from intercalation experiments performed on WO_3-based devices with WO_3 film thicknesses of 3850 Å, 1900 Å, 980 Å, and 490 Å. $V_a = -0.6$ V and $V_0 \approx 0.0$ V vs Ag/AgCl in aqueous electrolyte (0.01 N H_2SO_4); resistances are obtained from the initial currents for each curve

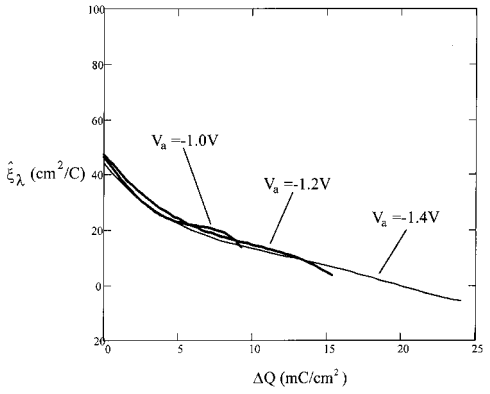

Fig. 12 The dynamic optical efficiency, $\hat{\xi}_\lambda$, vs the passed charge, ΔQ, for three values of the applied voltage ($V_a = -1.0, -1.2, -1.4$ V vs Ag/$AgNO_3$; $V_0 \approx -0.5$ V $\rightarrow -0.6$ V). The device is based on a 1800 Å WO_3 film in an Li-electrolyte (0.01 M $LiClO_4$ in dry propylene carbonate)

behavior. This should greatly facilitate device optimization and design.

Dynamic optical efficiency, $\hat{\xi}_\lambda$. The dynamic optical efficiency, $\hat{\xi}_\lambda$, is defined identically to that for the constant-current experiments (Eq. 3). The dynamic measurement, however, samples a wide variety of rates and represents the conditions and rate distribution present in actual device operation. Figure 12 shows the calculated $\hat{\xi}_\lambda$ as a function of the passed charge for four different applied voltages for an Li-intercalation system comparable to that used in the determination of ξ_λ (Fig. 4). It is seen that the curves coincide well with one another; application of an increasingly larger potential appears primarily to extend the curve.

For comparable ΔQ values, the data taken at higher potentials correspond to higher intercalation currents. The plot therefore suggests that no significant optically active processes occur with characteristic rates between those corresponding to the slowest- and fastest-rate curves (i.e., the curves corresponding to the lowest and highest applied overvoltages, respectively).

In comparing dynamic (constant voltage) with quasi-static (constant current) measurements, *one must restrict consideration to the potential range common to both*. If, in this range, $\hat{\xi}_\lambda$ is similar to ξ_λ, the dynamic process may be said to be occurring quasi-statically. In the present case, the initial potential corresponding to the dynamic measurements is between 0.5 and 0.6 V; relative to the quasi-static measurement, this corresponds to an initial ΔQ in the range of about 4 mC/cm^2 (this is obtained from the $V_{bi}(\Delta Q)$ characteristic for this system [3]). The meaningful comparison is then between $\xi_\lambda(\Delta Q + 4$ mC/cm$^2)$ and $\hat{\xi}_\lambda$, that is, one should compare Fig. 4 beginning at $\Delta Q \approx 4$mC/cm^2 to Fig. 12 beginning at $\Delta Q \approx 0$. It can be seen that, adjusting for the difference in initial conditions, $\hat{\xi}_\lambda$ and ξ_λ are of comparable magnitude, but the former is consistently and noticeably smaller than the latter.

Dynamic intercalation efficiency, $\hat{\zeta}$. It may be useful to define a dynamic intercalation efficiency, $\hat{\zeta}$, analogous to the quasi-static intercalation efficiency, ζ (Eq. 5). This requires a specific model, however, relating the current to the built-in potential and is therefore less phenomenological. For an ohmic current, the dynamic built-in potential is $\hat{V}_{bi} = V_a - RJ$, and $\hat{\zeta}$ is therefore given by

$$\hat{\zeta} = -\frac{\partial \Delta Q}{\partial RJ} \xrightarrow{R=\text{const}} -\frac{1}{R}\frac{\partial \Delta Q}{\partial J} \tag{12}$$

For an exponential current, one has $\hat{V}_{bi} = V_a - b \ln \frac{J}{a}$, and, for a and b constant, $\hat{\zeta}$ is given by

$$\hat{\zeta} = -\frac{1}{bJ}\frac{\partial \Delta Q}{\partial J} \tag{13}$$

In a general, phenomenological sense, it seems appropriate to use tacitly an ohmic model by taking the form of $\hat{\zeta}$ as determined by $-\frac{\partial \Delta Q}{\partial J}$. Multiplying by $1/R$ may then be performed to compare the scale to that obtained in quasi-static measurements. Figure 13 compares the quasi-static ζ vs V_{bi} with the ohmic-estimated dynamic $\hat{\zeta}$ vs $\hat{V}_{bi}$; R was taken as 300 Ωcm^2 for this calculation. It is seen that the scales match quite closely, but the forms are somewhat different.

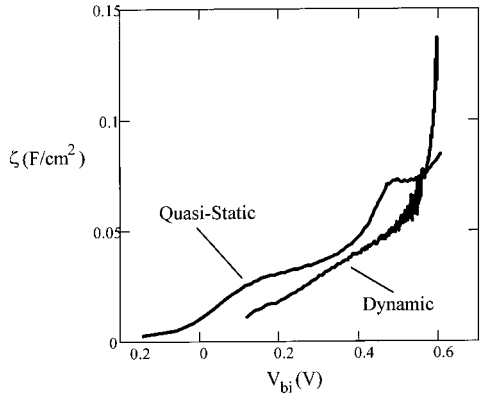

Fig. 13 Comparison of quasi-static and ohmic-estimated dynamic intercalation efficiencies for an aqueous system

Conclusions

A set of phenomenological analysis tools, referring only minimally to specific, mechanistic models, has been presented. These tools are intended for the characterization of optoelectrochemical behavior of electrochromic intercalation devices. Examples of such application are given for devices based on H- and Li-intercalation into tungsten oxide thin films.

The measured properties for a step current experiment are the time dependence of the applied voltage, $V_a(t)$, and of the transmission, $T(t)$; for a step potential experiment, one measures the time dependence of the electrical current, $j(t)$, and of the transmission, $T(t)$.

It has been demonstrated that investigation can often be performed in a state-space representation by considering the measured properties as functions of the passed charge, ΔQ, instead of the time, t. It has been shown that such a representation results in great simplification of scaling and shifting laws as well as providing a milieu for analysis which is far more intuitive and straightforward.

Step current measurements were shown often to give estimates of quasi-static properties. Quasi-static behavior often persists to unexpectedly high rates, including those associated with many step potential experiments.

Transmission curves ($T_\lambda(\Delta Q)$) may be used to obtain optical efficiency curves, which give a measure of how the sensitivity of the transmission to the passed charge varies with intercalation. Comparison of step current with step potential measurements can be used to estimate the extent to which quasi-static optical behavior persists.

Slow (quasi-static) step current measurements may be used to estimate the dependence of the built-in potential, V_{bi}, on the passed charge, ΔQ; knowledge of $V_{bi}(\Delta Q)$ is likely to form a cornerstone upon which specific, mechanistic models of the electrical behavior will be based.

With the presumption of a limiting mechanism, one can also estimate a dynamic built-in potential, $\hat{V}_{bi}$, from step potential experiments. If the mechanism assumption is correct, comparison with V_{bi} gives the degree to which the step potential electrical properties are behaving quasi-statically.

An intercalation efficiency, ζ, may be derived from a $V_{bi}(\Delta Q)$ curve. ζ is a measure of how the sensitivity of V_{bi} to intercalation varies with the intercalation level. Fine structure in ζ indicates the existence of distinct types of sites, separated significantly in energy; construction of a $\zeta(V_{bi})$ plot gives explicitly the energy distribution. Similarly, a dynamic intercalation efficiency, $\hat{\zeta}$, may be constructed from $\hat{V}_{bi}(\Delta Q)$.

Scaling and shifting properties with respect to several controlling variables have been derived and demonstrated for typical systems. This allows for the generation of master curves upon which data obtained under a variety of controlling conditions may be expected to collapse. Controlling variables investigated in this manner are initial device resistance, applied voltage, imposed current, and film thickness.

External modification of the overall device resistance may be brought about by placing resistors in series with the device. Study of $J(\Delta Q)$ curves obtained with a variety of series resistors may be used to investigate the controlling mechanism, since the mechanism determines the laws of collapse. This is also the case with variations in the applied voltage, but the former is often preferable because a similar range of intercalation level is sampled in each experiment.

Acknowledgements Financial support for the present work was provided by the Air Force Office of Scientific Research and by Donnelly Corporation. This support is gratefully acknowledged.

References

1. Granqvist CG (1995) Handbook of inorganic electrochromic materials. Elsevier, Amsterdam
2. Monk PMS, Mortimer RJ, Rosseinsky DR (1995) Electrochromism, fundamentals and applications. VCH, Weinheim
3. Denesuk M (1995) Electrical and optical behavior of tungsten oxide based electrochromic devices. PhD dissertation, University of Arizona, Tucson, Ariz (also available through UMI Dissertation Services, Ann Arbor, Mich)
4. Denesuk M, Cronin JP, Kennedy SR, Uhlmann DR (1997) J Electrochem Soc 144(3): 888
5. Denesuk M, Cronin JP, Kennedy SR, Uhlmann DR (1997) J Electrochem Soc 144: 1971
6. Denesuk M, Cronin JP, Kennedy SR, Uhlmann DR (1997) J Electrochem Soc 144: 2154
7. Heavens OS (1991) Optical properties of thin solid films. Dover, New York
8. Macleod HA (1989) Thin-film optical filters. McGraw-Hill, New York
9. Denesuk M, Cronin JP, Kennedy SR, Law KJ, Neilson GF, Uhlmann DR (1994) In: Wittwer V, Granqvist CG, Lampert CM (eds) Optical materials technology for energy efficiency and solar energy conversion XIII, vol. 2255, pp 52–61, SPIE Proceedings, Bellingham, Wash
10. Vuillemin B, Bohnke O (1994) Solid state ionics 68: 257–267
11. Bohnke O, Rezrazi M, Vuillemin B, Bohnke C, Gillet PA, Rousselot C (1992) Solar energy materials and solar cells 25: 361–374